Neuron, Vol. 48, 591–604, November 23, 2005, Copyright ©2005 by Elsevier Inc. DOI 10.1016/j.neuron.2005.09.034

The Temporal and Spatial Origins of Cortical Interneurons Predict Their Physiological Subtype

Simon J.B. Butt,[1,3] Marc Fuccillo,[1,3] Susana Nery,[1,4] Steven Noctor,[2,5] Arnold Kriegstein,[2,5] Joshua G. Corbin,[1,6] and Gord Fishell[1,*]

[1] Developmental Genetics Program
and the Department of Cell Biology
The Skirball Institute of Biomolecular Medicine
New York University Medical Center
540 First Avenue
New York, New York 10016

[2] Department of Neurology
and Center for Neurobiology and Behavior
Columbia University College of Physicians & Surgeons
630W 168th Street
New York, New York 10032

Summary

Interneurons of the cerebral cortex represent a heterogeneous population of cells with important roles in network function. At present, little is known about how these neurons are specified in the developing telencephalon. To explore whether this diversity is established in the early progenitor populations, we conducted in utero fate-mapping of the mouse medial and caudal ganglionic eminences (MGE and CGE, respectively), from which most cortical interneurons arise. Mature interneuron subtypes were assessed by electrophysiological and immunological analysis, as well as by morphological reconstruction. At E13.5, the MGE gives rise to fast-spiking (FS) interneurons, whereas the CGE generates predominantly regular-spiking interneurons (RSNP). Later at E15.5, the CGE produces RSNP classes distinct from those generated from the E13.5 CGE. Thus, we provide evidence that the spatial and temporal origin of interneuron precursors in the developing telencephalic eminences predicts the intrinsic physiological properties of mature interneurons.

Introduction

Cortical interneurons are key regulators of neuronal processing in the cerebral cortex and entrain numerous effects via a bewildering diversity of morphological and physiological subtypes. This diversity is a major stumbling block to elucidating the complexities of network function (Gupta et al., 2000; Klausberger et al., 2003; Reyes et al., 1998). One hope is that advances in genetic technologies will greatly facilitate our understanding of how interneuron populations function not only in vitro but in vivo as well (Monyer and Markram, 2004). One avenue of research that is particularly attractive is investigating how basic developmental processes contribute to interneuron diversity as defined in the mature network. This approach has as much to offer to developmental biologists, who are concerned with questions of cell specification and generation of cellular diversity, as it does to systems neuroscientists involved in the analysis of diverse cell types and their specific role in neuronal processing. In the mammalian spinal cord, ongoing studies have begun to correlate physiology with the fate-specific transcription factor code found in neural progenitors in the hope that such a link will provide a useful tool to further unravel the diversity and function of spinal neurons (Goulding and Pfaff, 2005; Kiehn and Butt, 2003; Sharma and Peng, 2001).

Local-circuit, inhibitory interneurons offer an excellent testament to the extent of neuronal diversity in the cortex; however, the various methods of classification have led to an often confusing picture (Markram et al., 2004). Initial studies in the guinea pig and rat identified relatively homogeneous populations of GABAergic interneurons (Kawaguchi, 1993; McCormick et al., 1985), but it is now apparent that there is a large diversity of cell types, classified according to their firing pattern in response to current injection, morphology, immunohistochemical content, and synaptic targets (Cauli et al., 1997; Gonchar and Burkhalter, 1997; Kawaguchi, 1995; Kawaguchi and Kubota, 1997; Markram et al., 2004; Somogyi et al., 1998). How this diversity relates to development is as yet unclear.

Fate-mapping experiments in mouse suggest that cortical interneurons are generated in the ventricular zone of the ventral ganglionic eminences and migrate tangentially into the developing cortex, in a process distinct from that involving the pyramidal projection neurons that are generated from the cortical ventricular zone (VZ) (Anderson et al., 2001; Nery et al., 2002; Wichterle et al., 2001). There is some evidence to suggest that these three ventral eminences (MGE, LGE, and CGE) represent a telencephalic correlate of the spinal cord progenitor domains, in which distinct sets of mature neurons are specified from an early time point in development. Similar to the spinal cord, these ventral eminences are marked by certain transcription factors that bestow a regional fate. A number of studies have suggested that within the ventral eminences there is segregation in the specification and fate of cortical interneuron phenotypes between the *Nkx2.1*-expressing medial ganglionic eminence (MGE) and the caudal ganglionic eminence (CGE) (Nery et al., 2002; Xu et al., 2004). However, little is known about how this early patterning relates to physiological classes defined at more mature ages. This is particularly difficult to address in the neocortex, as the perinatal lethality associated with null alleles of crucial patterning genes effectively prevents an

*Correspondence: fishell@saturn.med.nyu.edu

[3] These authors contributed equally to this work.

[4] Present address: London School of Hygiene and Tropical Medicine, Department of Infectious and Tropical Diseases, Unit of Pathogen Molecular Biology, Keppel Street, London WC1E 7HT, United Kingdom.

[5] Present address: DSCB Program, Department of Neurology, Box 0525, 513 Parnassus, HSW 1201, University of California, San Francisco, San Francisco, California 94143.

[6] Present address: Department of Neuroscience, Georgetown University, Georgetown University Medical Center, Room EP08, Research Building, Washington, District of Columbia 20057.

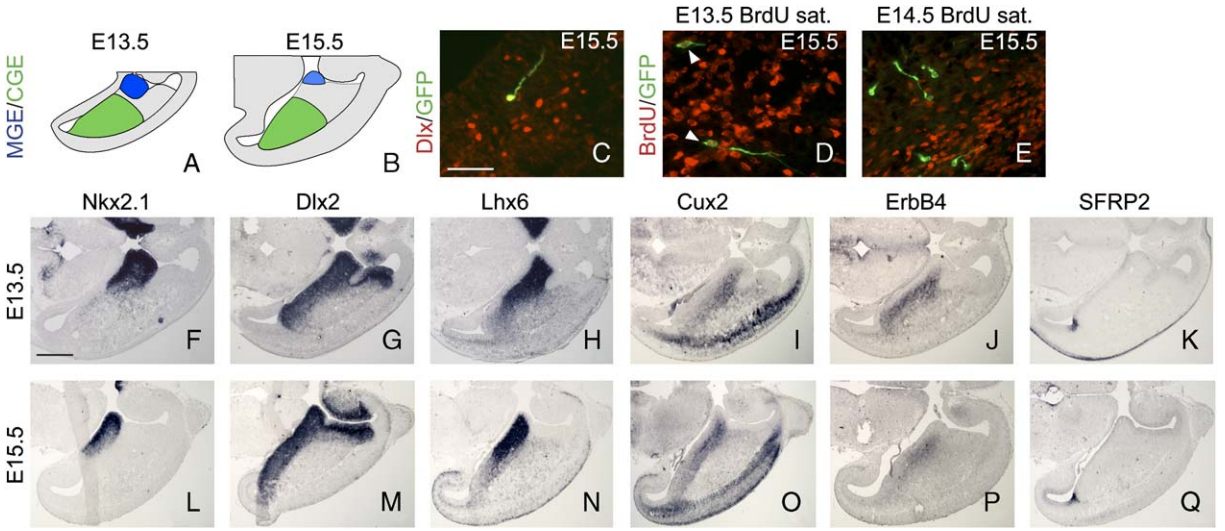

Figure 1. In Utero Fate-Mapping of the Ventral Telencephalic Eminences

(A and B) Schematic of the regions taken from the ventral telencephalon for in utero transplantation, as seen with the cortex removed and viewed from above. (C) Many transplanted progenitors expressed Dlx proteins, a characteristic of developing interneurons. BrdU saturation was performed immediately after transplantation (D) and 1 day following transplantation of MGE progenitors at E13.5 (E). Embryos sacrificed at E15.5 and stained with BrdU and GFP showed that while many progenitors proliferated immediately after transplantation (white arrowheads), after 1 day there were fewer proliferative transplanted neurons (E). The expression patterns of genes within the ventral eminences known to be involved in interneuron development are shown in horizontal sections at E13.5 (F–K) and E15.5 (L–Q), the two transplantation time points. Note that *Dlx2* expression extends throughout the ventral VZ/SVZ, but appears restricted due to the postmitotic mantle portion of the subpallium being negative for *Dlx2* expression. Scale bars: 50 μm (C–E), 500 μm (F–Q).

accurate analysis of the mature cell types that require these genes in vivo.

To address the question of whether a given source of cells in the developing ventral telencephalon is related to the physiology of the more mature system, we have performed electrophysiological, morphological, and immunocytochemical analyses of EGFP-fluorescent neurons in 2 to 3-week-old postnatal animals that have previously undergone in utero homotopic transplantation of either MGE or CGE progenitors. We provide evidence that the place and time of origin for interneurons in the developing ventral telencephalon predict their intrinsic physiological profile in the mature cortex.

Results

Cell Transplantation Techniques

Fate-mapping of ventrally derived cortical interneuron populations was made possible through the ultrasound backscatter microscopy (UBM)-guided cell transplantation techniques (Liu et al., 1998) previously employed by our lab (Nery et al., 2002; Wichterle et al., 2001). This technique has distinct advantages over in vitro systems for the analysis of the development of cortical interneuron subtypes. In vivo transplantation allows progenitor cells the opportunity to take their normal migratory pathways and integrate into the developing cortical plate in a physiologically relevant manner. This is an especially important consideration given that these eminences also contribute to numerous other structures including the striatum, the amygdala, and the nucleus accumbens (Wichterle et al., 2001; Nery et al., 2002; Xu et al., 2004). Moreover, our in vivo approach allows these cells to be analyzed upon their normal in situ maturation. Although UBM-guided injections allow for the accurate placement of transplanted neurons (Liu et al., 1998), our previous work has demonstrated that the source of the donor tissue is the primary determinant of the migration pattern and final position of grafted cells (Wichterle et al., 2001; Nery et al., 2002).

The E13.5 MGE and CGE progenitor domains were dissected as shown in Figure 1A with the interganglionic sulcus used as the major anatomical landmark to demarcate the posterior end of the MGE. In keeping with previously proposed boundaries (Nery et al., 2002), a small portion of the anterior CGE was *Nkx2.1*-positive (compare Figures 1A and 1F). Transplantation of E15.5 progenitors was performed only for the CGE, as targeting of the MGE with UBM imaging was not reliable at this stage, owing to its reduced size. Tissue for E15.5 CGE (Figure 1B), as well as the more restricted *d*CGE transplants, was taken entirely from an *Nkx2.1*-negative region, as tested by whole-mount in situ hybridization of representative tissue pieces (data not shown).

Transplanted cells seem to behave normally at both short- and long-term time points, as judged by their morphology and pattern of migration. Tangentially migrating EGFP-positive progenitors were also observed to have Dlx immunoreactivity, indicating that they were progressing through a normal interneuron maturation program (Figure 1C) (Anderson et al., 1997). The proliferative capabilities of transplanted cells were assessed by saturation BrdU labeling (three injections of 1 mg/10gm mother, every 4 hr) of the host mothers at three time points: during surgical recuperation, 1 day after, and two days after E13.5 transplantation. Analyzed at E15.5, a subset of transplanted progenitors continues to proliferate to a limited extent one full day after being placed in the embryonic brain (see Figures 1D and 1E). The patterns of various transcription factors linked to interneuron

development are shown in Figures 1F–1Q for comparison to the underlying transplantation scheme employed in fate-mapping. *Nkx2.1* and *Dlx2* transcripts are largely expressed in VZ/SVZ progenitors (Figures 1F, 1G, 1L, and 1M), while *Lhx6*, *Cux2*, and *ErbB4* mRNAs are expressed in the postmitotic mantle and remain on in tangentially migrating neuronal precursors at later stages (Figures 1H–1J and 1N–1P) (Flames et al., 2004; Lavdas et al., 1999; Zimmer et al., 2004). *SFRP2* was employed as a marker of the posterior extent of the CGE at both E13.5 and E15.5 time points (Figures 1K and 1Q).

Electrophysiology

EGFP-positive cells were distributed throughout the full anterior-posterior extent of the juvenile (P13–P22) cortex, as previously reported (Nery et al., 2002; Wichterle et al., 2001). We recorded from a total of 171 EGFP-positive profiles (n = 50, E13.5 MGE transplant; n = 54, E13.5 CGE; n = 37, E15.5 CGE; n = 30 E13.5 *d*CGE) from layers 2–6 of the somatosensory cortex. All recorded neurons had electrophysiological properties and morphologies consistent with their being interneurons (Kawaguchi, 1995; Kawaguchi, 1993). EGFP-positive interneurons exhibited robust spontaneous synaptic activity and normal passive and active membrane properties similar to findings in published data as well as in a number of non-EGFP control interneuron recordings (n = 56; data not shown), indicating that homotopic transplant of interneuron progenitors at early embryonic ages does not adversely affect their maturation and final integration into the cortical circuitry.

During the course of our study and across the varying transplants, we identified cells with the characteristics of four main cortical interneuron subclasses (Kawaguchi and Kubota, 1997): fast-spiking (FS) and late-spiking (LS) interneurons as well as burst-spiking (BSNP, also known as low-threshold [LTS] interneurons), and regular-spiking (RSNP) nonpyramidal cells. However, there were pronounced differences between MGE and CGE in the number of each class of cell when transplanted at E13.5 and also between CGE tissue transplanted at E13.5 and that transplanted at E15.5.

E13.5 MGE Transplants

Homotopic transplants of cells from the E13.5 MGE resulted in a significant number of EGFP-positive profiles in the somatosensory cortex (typically 30 or more viable cells per 200 μm slice) that were biased toward the deeper layers. In total, we recorded 50 cells from the MGE, of which 19 were located in layers 2 and 3 and the remainder were in the deeper layers. Thirty-seven cells were recovered for histological analysis. The predominant mature interneuron phenotype recorded in all layers from MGE transplants belonged to the fast-spiking (FS) class. These accounted for 54% of the interneurons from that region and exhibited classical properties of fast, repetitive action potentials with little or no adaptation during suprathreshold depolarizing current steps (Figure 2A) (Kawaguchi, 1993; McCormick et al., 1985). In addition, they exhibited large, fast afterhyperpolarizations (AHP), significantly hyperpolarized resting potentials (resting membrane potential [RMP] = −67.1 mV ± 4.6; n = 27), lower input resistances (R_{in} = 288.9 MΩ ± 138.7), and faster time constants (tau [τ] = 16.1 ms ± 7.8) relative to the other types of interneurons recorded from MGE transplants (Figure 2B; see also Table S1 in the Supplemental Data available with this article online). The morphologies for 21 of the FS cells were recovered, of which three had three to four prominent dendrites ramifying deep into layer 1 and an axon branching in the immediate vicinity in layer 2 with cartridges typical of FS chandelier cells (Figure 2D) (Kawaguchi, 1995; Somogyi, 1977). The remaining 18 had basket cell morphologies: multipolar with smooth dendrites and axons originating from the soma (Figure 2C). The majority had a dense local axonal plexus (n = 14), whereas a few had elongated horizontal collaterals typical of wide-arbor basket cells.

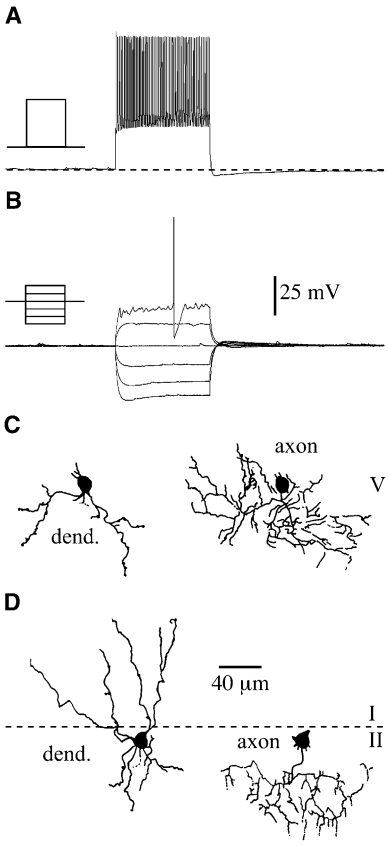

Figure 2. Fast-Spiking (FS) Interneurons Are the Principal and Exclusively MGE-Derived Population at E13.5

(A) Response of a FS interneuron to a 1.05 nA, 500 ms current step. FS interneurons exhibited fast, repetitive action potentials in response to suprathreshold current injection. (B) Subthreshold and threshold responses of an FS interneuron to depolarizing and hyperpolarizing current steps (steps starting at −0.15 nA with 0.05 nA increments; duration, 500 ms). Near-threshold current steps often elicited small amplitude oscillations in the voltage response. (C) Reconstruction of an FS interneuron with smooth beaded dendrites (dend.) and an axon originating from the soma with a dense innervation local to the soma, typical of basket cell morphology. (D) Layer 2 FS interneuron with thick dendrites projecting into layer 1 and axon with cartridges characteristic of chandelier cell morphology.

The second largest population was that of the regular-spiking nonpyramidal (RSNP) cells, which accounted for 20% of the E13.5 MGE transplant population (n = 10). Within this class there were two distinct subpopulations (see also Cauli et al., 2000). The first, which we termed

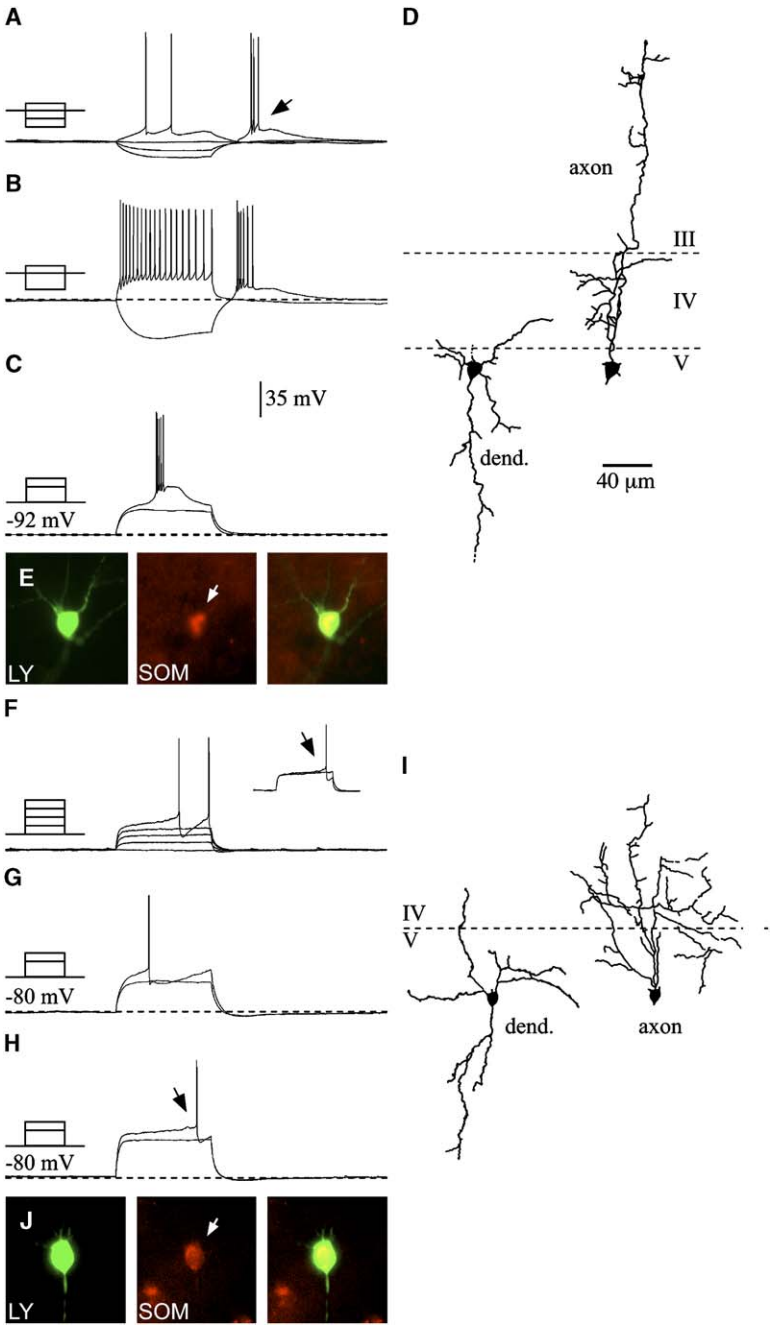

Figure 3. Somatostatin-Positive Burst-Spiking Nonpyramidal (BSNP) and Delayed-Spiking (DS) Interneuron Populations Are Common to Both MGE and CGE E13.5 Transplants

(A–E) Electrophysiological and histological profile of layer 5 BSNP. (A) BSNPs fired a burst of two or more action potentials (arrow) in response to hyperpolarizing current injection and more regular action potentials in response to small depolarizing current steps (initial step, −20 pA with 10 pA increments; duration, 500 ms). (B) A large hyperpolarizing current step (−60 pA) resulted in prolonged bursts of up to seven to ten spikes. Depolarizing current injection (+90 pA) to near-maximal firing frequency resulted in adaptation in spike frequency. (C) BSNPs also exhibited bursts of action potentials in response to depolarizing current steps from a steady-state hyperpolarized potential (subthreshold step, +60 pA; threshold, +70 pA). (D) Reconstruction of the morphology of the same cell as in panels (A)–(C), with Martinotti-like characteristics. (E) Lucifer yellow (LY)-filled BSNPs were immunopositive for antibodies against the peptide somatostatin (SOM), as indicated by the arrow. (F–J) Profile of a class of late-spiking interneurons termed delayed-spiking (DS) interneurons. (F) Steps increasing by 20 pA (500 ms, 0.2 Hz) each time revealed a delay to spike that was more apparent at threshold (inset, arrow; step to +80 pA and +82.5 pA) and due to a slow ramp depolarization. (G) When depolarized from a hyperpolarized holding potential, the ramp and associated delay to spike were not so prominent (step to +100 pA, +120 pA) unlike in the three classical late-spiking, neurogliaform neurons recorded (+150 pA, +180 pA) (H). (I–J) The morphology and immunoreactivity of DS interneurons were more consistent with BSNPs (D). The example shown was multipolar, with sparsely spiny dendrites and an axon originating from the pial surface and ascending into, and ramifying in, the immediate layer above. In addition, DS interneurons were immunopositive for somatostatin (SOM).

rebound (R-) RSNPs, exhibited a single rebound spike on release from a hyperpolarizing current step and depolarized resting potential (−57.3 mV ± 1.7; n = 4) (Figures S1A and S1B). The second population of RSNPs exhibited no rebound spike (NR-RSNPs), a more hyperpolarized resting potential (−61.2 mV ± 1.7; n = 6) and often a prominent notch in the AHP (Figures S1C and 1D). R-RSNPs were located deep in layer 5/6 or at the border of 1/2 and were multipolar with aspiny dendrites and an ascending axon originating from the pial side of the soma that branched in the layers above (data not shown). The NR-RSNPs recovered were located in layer 2 and had extensive dendrites projecting laterally and downward into layer 3 (Figure S1E). Similar to the R-RSNPs, the axon originated from the soma and branched extensively before entering layer 1; all tested negative for calretinin. The firing pattern, location, and axonal arbor of these NR-RSNPs are similar to those described for a population of somatostatin-positive RSNPs (Cauli et al., 1997; Kawaguchi and Kubota, 1996).

Of the classical interneuron subtypes, the next largest population was that of the burst-spiking interneurons (BSNPs; n = 6). All of these exhibited a burst of two or more spikes on rebound from a hyperpolarizing current step, as well as multiple spikes at threshold when depolarized from a hyperpolarized holding potential (Figures 3A–3C) (see Kawaguchi, 1995). They had relatively depolarized resting potentials (−55.2 mV ± 7.4; n = 6), high input resistances, slow time constants, and a high percentage of spike-frequency adaptation (Table S1).

The majority (four of six) were located in layer 5/6, and three tested positive for an antibody against somatostatin (Figure 3E). All of the cells had a Martinotti morphology with three to four sparsely spiny primary dendrites that were confined to the same layer, or the immediately adjacent layer, as the soma but with an ascending axon that originated from the soma and projected to the superficial layers (Figure 3D).

During the course of our experiments, we also encountered a population of cells that we initially classified as late-spiking (LS) interneurons, based on a pronounced delay to spike at threshold due to an underlying slow ramp depolarization when stepped from resting membrane potential (Figure 3F) (n = 6 from E13.5 MGE). However, the delay to spike was attenuated (<150 ms) when the cell was depolarized from a hyperpolarized holding potential (<−80 mV) (Figure 3G as compared to classical LS interneurons, Figure 3H). Given that this type of cell was distinct from the LS class previously described, we have termed them delayed-spiking (DS) interneurons. In all other aspects they resembled NR-RSNPs and did not exhibit a rebound spike in response to hyperpolarizing current injection (data not shown). All the cells recovered were in the upper portion of either layer 2 or layer 5 and had a distinctive morphology that was not typical of the LS-neurogliaform class previously described (Kawaguchi, 1995). In all cases they had two laterally projecting dendrites from the pial side of the soma and additional processes, including usually one or two prominent, sparsely spiny dendrites descending deep into layer 3 or layer 6 (Figure 3I). The axon projected dorsally, with processes in some cases extending to layer 1. All had axons that branched extensively, directly above the soma in either layer 1 or 4. Immunocytochemistry identified this population as somatostatin-positive and in this, as well as morphologically, they resembled a population of Calbindin D_{28k}, somatostatin-positive BSNP cells previously described (Kawaguchi and Kubota, 1996) (Figure 3J).

E13.5 CGE Transplants

Transplant of E13.5 CGE progenitors resulted in fewer cells in the postnatal cortex than seen with MGE progenitors (usually <20 cells per 200 μm slice). Furthermore, the cells were preferentially distributed in the more superficial layers (34 of 54 cells). Notably, of the 54 cells recorded, none were of the FS interneuron class, which forms the bulk of the MGE-derived cells at the same time point (for the full electrophysiological data set, see Table S2). As observed in the MGE transplants, CGE transplants also gave rise to BSNP (22% of the overall E13.5 CGE population) and DS interneurons (9%). Each of these classes of interneurons resembled in all aspects those recorded from the MGE transplants.

The bulk of the CGE-derived cells were of the RSNP class (63%, n = 34) (Figure 4) and among them, the dominant subtype was that of the NR-RSNP class (41% of the overall sample; n = 22). Unlike the MGE NR-RSNPs, those from the CGE represented a more diverse population in terms of both their physiological and histological properties (Figures 4A–4D). Overall, they were defined by the lack of a rebound spike after a hyperpolarizing current step, hyperpolarized resting potentials (−63.0 mV ± 6.9; n = 22), and adaptation in spike frequency (48.4% ± 20.3; n = 22). A number of distinctive subclasses were evident, two of which were unique to E13.5 CGE transplants: (1) a group consisting of eight cells that exhibited a marked adaptation in spike frequency and amplitude in the early part of the depolarizing current step (Figure 4A; see RSNP-VIP class, [Cauli et al., 2000]) as well as small, local plexus morphologies either at the border of layers 1 and 2 or deep in layer 5/6 (Figure 4B); and (2) a population (n = 4) that had a firing pattern resembling that previously reported for a parvalbumin-expressing population of layer 2 cells (Blatow et al., 2003) in that supraspike threshold current injection elicited a burst of two or three spikes followed at a delay by regular spiking (Figure 4C). However, these cells were distinctive from those previously reported in that although they were located in layer 2, they had bitufted morphologies similar to another VIP-expressing population reported by Rozov et al. (2001) with aspiny dendrites projecting to the pial surface as well as ventrally to layer 5 (Figure 4D). The axon originated from the soma and branched in the immediate layer below the soma. Of the remaining 10 cells, four were distinctive in that they had small spherical soma and were bipolar with the axon extending off the descending dendrite (data not shown). In addition, they also displayed pronounced adaptation in spike frequency (61.3% ± 27.6; n = 4) and a long-duration (>2.5 s) slow AHP (sAHP) after the end of supraspike threshold current steps. This cell class was evident in greater numbers from E15.5 CGE transplants (see below).

The R-RSNPs fell into two groups principally on the basis of their morphology: (1) calretinin-immunopositive bipolar interneurons with axons originating from the descending dendrite (Figures 4E–4G); and (2) multipolar, somatostatin-positive sparsely spiny interneurons with ascending axons originating from the soma (Figures 4H–4J). Physiologically, the former exhibited marked inward rectification in the subthreshold voltage responses, little or no depolarizing sag in voltage during hyperpolarizing current steps indicative of the hyperpolarization-activated potassium current (I_h), and a slow time course to the rebound spike after the end of the hyperpolarizing current step (Figure 4E). The latter showed the opposite: little or no rectification, sizeable (>3 mV when stepped to approximately −100 mV) voltage sags due to I_h, and an abrupt rebound spike after the end of the negative current step (Figure 4H).

In addition to these main cell classes, we also recorded two calretinin-positive irregular-spiking interneurons (IS) and a single neurogliaform LS interneuron.

Immunohistochemical Analysis of E13.5 Transplanted Progenitors

To complement the whole-cell electrophysiological analysis of EGFP-positive neurons in the somatosensory cortex, we performed a larger, population-based assay of the expression of a panel of interneuron markers on cryosectioned P21 mouse brains from E13.5 MGE and CGE transplants. These immunological markers consist of calcium binding proteins (parvalbumin, calretinin, and calbindin), voltage-gated potassium channels (Kv3.1 and Kv3.2), and other neuromodulatory substances (neuropeptide Y [NPY], somatostatin [SOM], and vasointestinal peptide [VIP]). Classification schemes based on

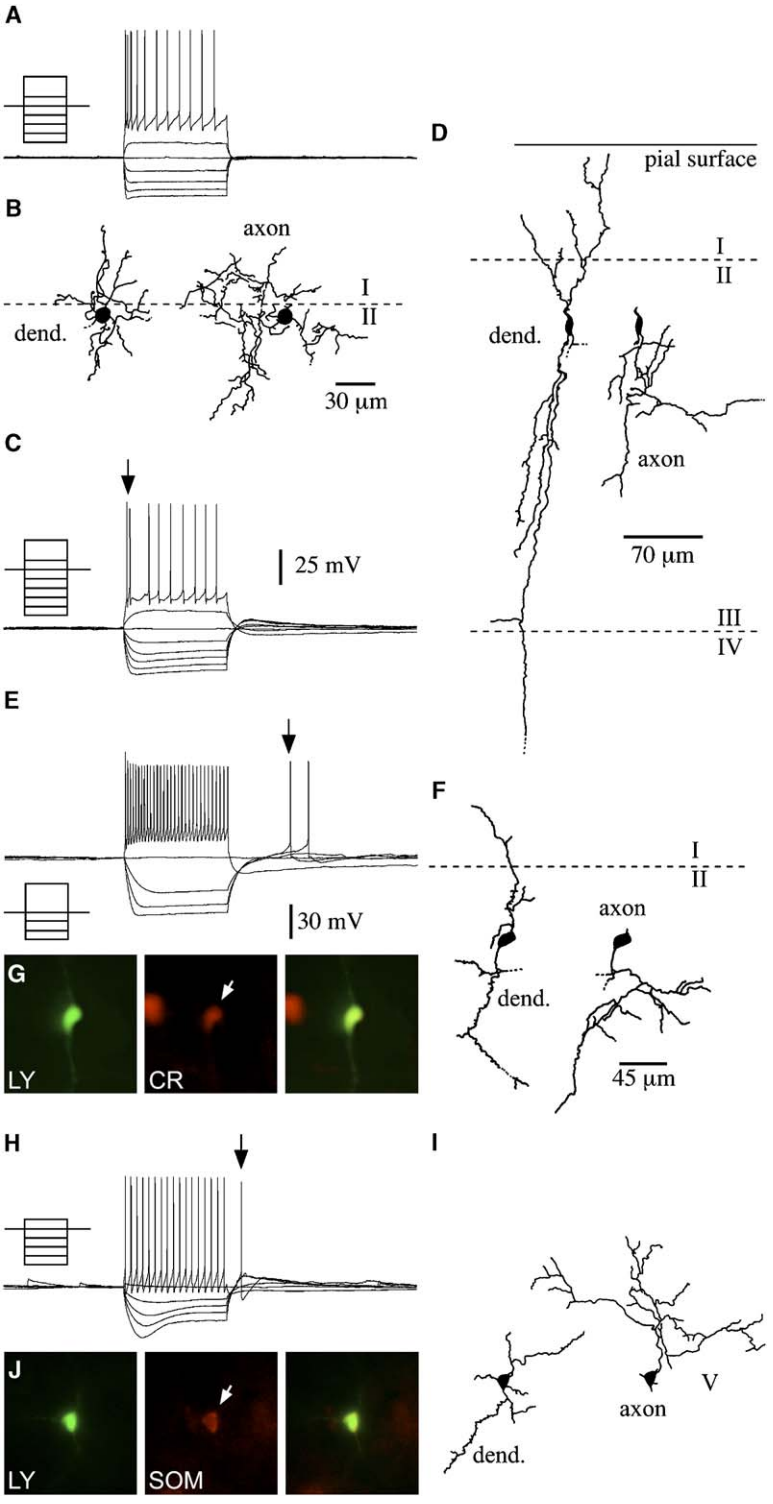

Figure 4. Regular-Spiking Nonpyramidal (RSNP) Neurons Account for the Majority of Cells Recorded from E13.5 CGE Transplants

(A–D) Subtypes of E13.5 CGE-specific RSNPs. (A and B) A class of NR-RSNP that exhibited adaptation in the initial phase of firing (−200 pA, 50 pA) and a dense plexus morphology. (C and D) Physiological and morphological characteristics of a class of bitufted layer 2 interneurons that fired a burst of two to three spikes (C, arrow) followed at a delay by regular firing (−100 pA initial step with 20 pA increments). (E–J) Rebound (R-) RSNPs were defined on the basis of their firing a single action potential on rebound from a hyperpolarizing step (indicated by the arrows in panels [E] and [H]). Two distinct subtypes were evident (see Results for details). (E) Firing pattern (initial step, −60pA with 20 pA increments to 0 mV; suprathreshold current injection of +120 pA) of the bipolar (F), calretinin-positive (CR; panel [G]) R-RSNP subtype. (H–J) Profile of the multipolar, somatostatin (SOM) R-RSNP class.

analysis of the aforementioned markers are sometimes hampered by the lack of specificity of available markers for particular electrophysiological subclasses of interneurons (Kawaguchi and Kubota, 1997; Markram et al., 2004). Nonetheless, our single-cell analysis made several predictions about the immunological profiles of transplantation cohorts that could be tested on a more global level.

Fast-spiking interneurons are known to express the delayed-rectifier potassium channel Kv3.1 (Du et al., 1996). Expression of this channel is required for the rapid repolarization of the action potential and underlies the rapid, nonadapting firing pattern characteristic of these interneurons (Erisir et al., 1999). A similar channel, Kv3.2, overlaps largely with Kv3.1 in deep layer fast-spiking neurons, but is only expressed at low levels in

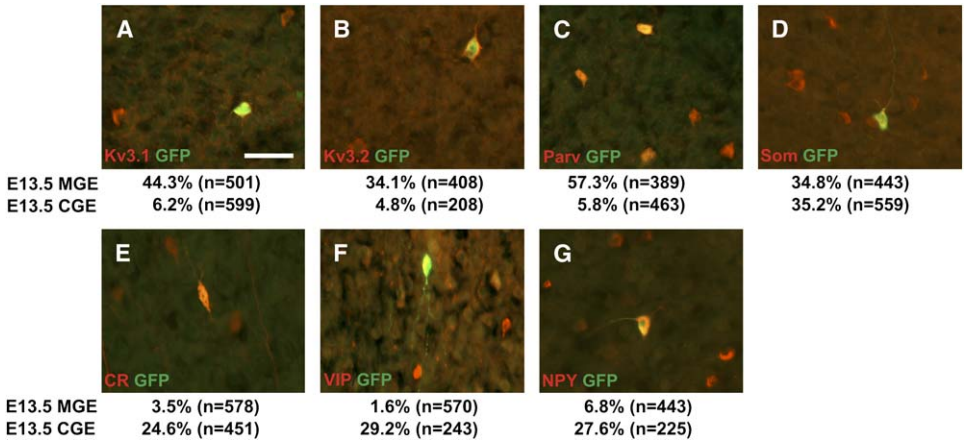

Figure 5. Immunological Characterization of E13.5 MGE and CGE Transplants

(A–G) Immunocytochemical colabeling of GFP, to mark transplanted cells, and a number of mature interneuron markers on P21 cortical cryosections. All percentages are expressed as the number of marker-positive cells per GFP-positive transplanted pool counted within the somatosensory cortex. Markers indicative of the fast-spiking phenotype, including Kv3.1, Kv3.2, and parvalbumin (A, B, and C, respectively) were at least 7-fold greater in E13.5 MGE transplants in comparison to E13.5 CGE transplants. Somatostatin-positive profiles were equally distributed between both eminences (D). Conversely, calretinin, VIP, and NPY (E, F, and G, respectively) were strongly biased toward CGE transplants. Scale bar, 30 μm.

superficial cells and is also present in a subset of non-fast-spiking neurons (Chow et al., 1999). Parvalbumin has been reported to be expressed by most, if not all, FS cells and shows a high degree of overlap with Kv3.1 and Kv3.2 (Chow et al., 1999); however, it is also present in a class of non-FS interneurons (Blatow et al., 2003). Immunological analysis with this panel of markers corroborated the electrophysiological results in that MGE transplanted cells gave rise to interneurons with immunological profiles consistent with the FS subclass (Figures 5A–5C). Forty-four percent of the transplanted GFP-positive neurons costained with Kv3.1, while 34% were Kv3.2 positive, probably reflecting the more restricted pattern of Kv3.2 expression. Likewise, 57% of MGE transplanted cells expressed parvalbumin. In contrast, the CGE transplanted neurons showed virtually no fast-spiking immunological profiles, with 6.2% Kv3.1, 4.8% Kv3.2, and 5.8% parvalbumin expression.

The neuropeptide somatostatin is expressed in some subclasses of RSNPs, but is consistently found in deep layer BSNP cells with Martinotti morphology (Kawaguchi and Kubota, 1996), a subclass that was observed equally in both E13.5 MGE and CGE. Somatostatin expression was roughly equal between both E13.5 cohorts at approximately 35% (Figure 5D). The large representation of RSNP subclasses from the E13.5 CGE electrophysiological analysis was paralleled by the array of immunological markers observed in these subgroups. The most specific markers for this eminence were the calcium binding protein calretinin and the neuropeptide VIP, which is sometimes coexpressed with calretinin (Kawaguchi and Kubota, 1997). Both of these markers were preferentially expressed in the E13.5 CGE cohort compared to their expression in the MGE: 24.6% versus 3.5% for calretinin and 29.2% versus 1.6% for VIP, respectively (Figures 5E and 5F). Neuropeptide Y is expressed by a subset of interneurons that are mainly localized to superficial cortical layers, particularly the layer II/I boundary, as well as some deep layer cells. Despite previous work suggesting that NPY neurons were exclusively MGE-derived (Anderson et al., 2001), our experiments showed that NPY was found at a 4-fold higher frequency in CGE versus MGE transplants (Figure 5G; see also Figure S3).

E15.5 CGE Transplants

To ascertain whether there is a shift in the physiological properties of the interneurons produced by the eminences over time, we undertook transplants of E15.5 CGE precursors. Due to the reduction in size of the MGE at this age (Figures 1A and 1B), it was not possible to reliably perform transplants of this region. In total we recorded 37 EGFP-transplanted neurons in the somatosensory cortex (24 were recorded in superficial layers), all of which were interneurons (see Table S3). Similar to the E13.5 CGE, the main class of interneurons at the later time point were of the RSNP class (n = 17; 46%) and of those, the majority were NR-RSNPs (12 of 17). However, there was considerable variation in the subtypes observed between the two time points. We did not record from any of the dense plexus or bitufted neurons that comprised two of the distinctive NR-RSNP populations derived from the earlier born neurons. Instead, we identified two main types of cell, both of which exhibited slow, regular firing (compared to FS cells) at just above spike threshold. One subtype (n = 6) continued to fire in a fairly regular manner (data not shown), whereas the other (n = 6) showed pronounced, rapid adaptation in spike frequency (95.4% ± 7.4) in response to large depolarizing current steps and a long-duration sAHP (Figures 6A–6C). All of the cells in this latter class were located in layer 2 and had either bipolar, bitufted, or double bouquet morphologies with axons off the descending dendrite (Figure 6D). As such, they corresponded to the population of rapidly adapting RSNPs recorded from E13.5 transplants. The regular firing cells were multipolar with sparsely spiny dendrites and the axon originating from the soma.

An additional group of RSNPs (n = 5) also exhibited rapid adaptation in spike frequency, prolonged sAHP,

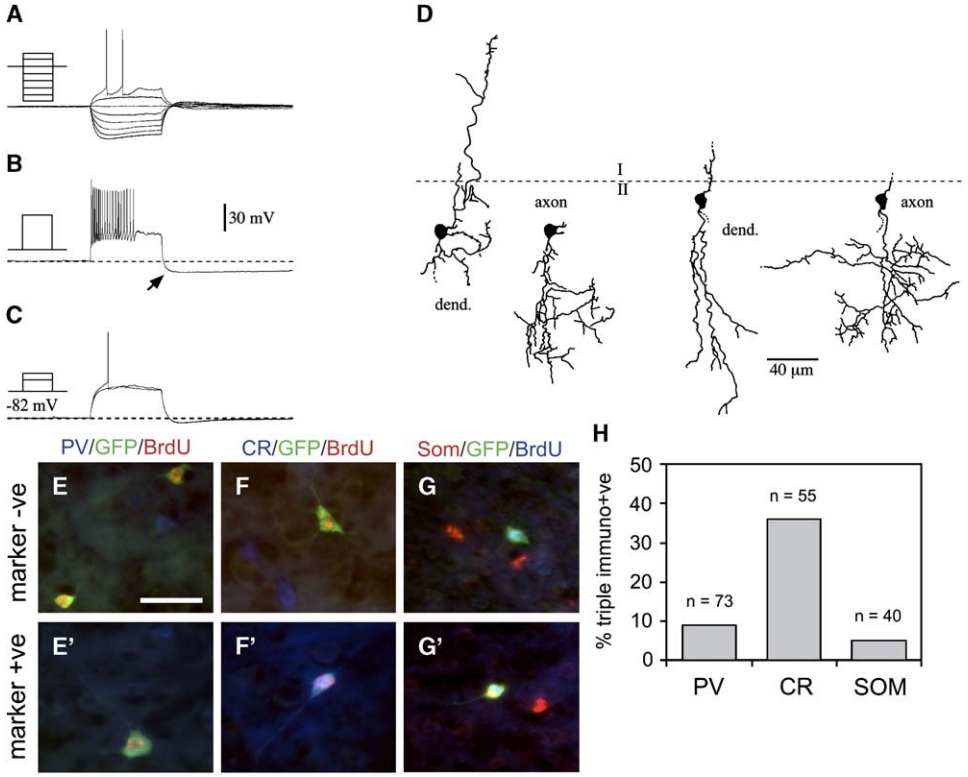

Figure 6. Rapidly Adapting RSNPs with Mainly Bipolar Morphologies Were Characteristic of E15.5 CGE Transplants

(A) Subthreshold voltage response of a rapidly adapting NR-RSNP (−75 pA, 15 pA steps). (B) The cell exhibited pronounced adaptation and failure of spikes in response to large depolarizing current injection and a pronounced slow afterhyperpolarization (sAHP) (arrow) (+120 pA step). (C) Although these cells fired in a burst-like manner in response to depolarizing current injection, they were characterized as RSNPs as they only fired a single spike in response to depolarizing current injection from a hyperpolarized holding potential (+55 pA, +60 pA steps). (D) Two examples showing the vertically orientated morphologies typical of rapidly adapting RSNPs. In all cases the axons originated off dendrites and predominantly from the descending dendrite in bipolar interneurons (right). Axons arborized in the layer immediately below the soma but in some cases had ascending collaterals (data not shown). (E–G') Proliferating E15.5 ventral progenitor zones were labeled with BrdU prior to removal and transplantation of CGE. Cryosections of transplanted P21 brains were stained with antibodies to GFP and BrdU, to mark transplanted cells that originated within the CGE ventricular zone, as well as another marker of broad interneuron subclass. (E)–(G) show representative examples of E15.5 CGE-derived transplanted neurons that are negative for the three respective interneuron markers. (E')–(G') show representative examples of triple labeling. (H) Percentage data are summarized in the histogram. These data suggest that a large number of calretinin-positive interneurons are derived from the E15.5 CGE ventricular zone, while this region generates smaller numbers of parvalbumin and somatostatin-expressing interneurons. Note that for technical reasons, BrdU is found on the blue channel only in conjunction with somatostatin staining. Scale bar for (E)–(G), 30 μm.

and bipolar morphology, but were classified as R-RSNPs because a rebound spike was elicited in response to a hyperpolarizing current step ≥ -90 mV. In contrast to the bipolar R-RSNPs from E13.5 CGE, these neurons did not show marked inward rectification and had a sizeable sag in voltage due to I_h (6.7 mV ± 5.2) as well as a fast depolarizing notch associated with the rebound spike (data not shown).

The second largest population from the E15.5 CGE transplants was the FS interneuron class previously associated only with MGE transplants (n = 14; 38%). They were indistinguishable from those of the MGE with regard to all of the physiological parameters measured. Morphologically they comprised predominantly small arbor basket cells with no wide arbor basket or chandelier cells evident. This later CGE population also differed from both the earlier transplants in that no BSNPs were recorded, though other minor classes observed included DS (n = 4) and LS (n = 2) interneurons. Immunohistochemical analysis of E15.5 CGE transplants was generally consistent with the electrophysiological analysis (Figure S3).

Identification of Caudal Migrating Interneuron Populations

The preponderance of CGE-derived FS cells suggested either contamination of the E15.5 CGE with progenitors migrating from different regions or a progressive maturation model of interneuron cell fate, whereby the ventral eminences passed through anterior-posterior (A-P) waves of differentiation, each giving rise to a specific cell type in different time windows. Support for the former came from examination of E13.5 MGE transplants at E15.5, which showed enormous dispersion of migrating cells to the most posterior regions of the ventral eminences, an observation largely supported by expression patterns of *Lhx6*, whose expression serves as a marker of cell migration from the MGE (Anderson et al., 2001; Lavdas et al., 1999) (Figure S2 and Figures 1H and 1N). To further investigate the source of these E15.5 FS cells, we carried out a modified version of the E15.5 transplantation protocol in which ventricular zone progenitors were labeled with a BrdU pulse 3 hr prior to sacrifice of the EGFP donor embryos. We assumed that MGE-derived postmitotic cells migrating through the CGE at

this time point would not be labeled by a BrdU pulse. The BrdU pulse length was adjusted to maximize CGE ventricular zone labeling while minimizing the possibility of collecting MGE cells that had taken up BrdU and subsequently migrated into the CGE.

Sections of transplanted brains were made at P21, then stained for GFP to mark transplanted cells, BrdU to label cells originating from the CGE proliferative region, and parvalbumin, somatostatin, or calretinin (Gonchar and Burkhalter, 1997). The percentage of GFP/BrdU double-positive cells that expressed one of these three general interneuron markers was used to approximate the interneuron subtypes generated directly from the E15.5 CGE ventricular zone. Parvalbumin triple labelings represented 9% of BrdU/GFP-positive transplanted neurons, while somatostatin triple labelings accounted for 5% of the BrdU/GFP population (Figures 6E and 6G). In contrast, 36% of the BrdU/GFP-positive population coexpressed calretinin (Figure 6F). This approach suggested that few if any parvalbumin- and somatostatin-positive cells were generated from the E15.5 CGE while calretinin-positive neurons represented a much larger portion of CGE-derived cells at this time point. Thus, it is likely that the FS interneurons recorded in our electrophysiology sample at E15.5 originated in the MGE.

E13.5 Dorsal CGE Transplants

The fact that caudally migrating interneurons are present within the E15.5 CGE donor tissue raised the possibility that MGE-derived cells may also be present within the CGE at the earlier E13.5 time point. Indeed, the presence of both *Nkx2.1* and *Lhx6* in our E13.5 CGE donor tissue makes this seem quite probable (Figures 1F and 1H). To investigate this and to determine specifically which populations originate within the CGE itself at this age, we performed E13.5 transplantations of a restricted, dorsal portion of the CGE, which we term *d*CGE. The boundaries of the region used in these refined CGE transplants are indicated in the diagram shown in Figure 7A. This region encompassed the dorsal aspect of the CGE ventricular zone and underlying mantle, but not the more medial, ventral CGE region that contains the caudal tail of *Nkx2.1* and *Lhx6*-expression (Figure 7A). To confirm that transplanted cells originated within the *d*CGE ventricular zone, we BrdU-pulsed donor animals 3 hr prior to isolating tissues for transplantation. In addition, to ascertain that the mature physiological character of these cells was cell-autonomously specified at the time of transplantation, we also heterotopically transplanted *d*CGE donor tissue into the MGE in a subset of experiments.

We recorded a total of 30 interneurons from P14–P18 animals that had undergone in utero transplantation. Of these, 20 of the cells recorded were from homotopic transplants, while the remaining ten were from animals in which the *d*CGE was heterotopically injected into the MGE. All ten cells had properties not found in MGE transplants but consistent with their being CGE interneurons—in agreement with previous studies suggesting that the source of the donor tissue is the primary determinant of cell fate (Wichterle et al., 2001; Nery et al., 2002). As there was no apparent difference noted between these samples, we have pooled the electrophysiological data in our Results section. Of the 30 interneurons, the vast majority (80%) were RSNPs, consistent with those found in our previous E13.5 CGE transplants (Figure 7; Table S4). In addition, no fast-spiking (FS) interneurons were recorded. One notable difference between the E13.5 *d*CGE and CGE samples was that only a single BSNP (*d*CGE: 3%; CGE: 22%) and no DS interneurons (*d*CGE: 0%; CGE: 9%), two of the main somatostatin-positive populations previously recorded from E13.5 transplants, were recorded. Overall, of the 29 interneuron morphologies recovered, the majority (n = 13) had bitufted, bipolar (Figures 7B, 7F, and 7J), or double bouquet arbors, while a smaller number were multipolar and included a type similar to sparsely spiny VIP-positive arcade cells (Figure 7I) (Kawaguchi and Kubota, 1996). The remaining cells corresponded to the dense plexus, rapidly adapting RSNP population specific to the E13.5 CGE sample. Analysis of the immunohistochemical profile of *d*CGE interneurons also revealed a significant drop in the number of somatostatin-positive neurons; however, the proportions of calretinin, VIP, and NPY-labeled GFP interneurons remained high (Figures 7B and 7C). Moreover, 25% of the transplanted *d*CGE cells that incorporated into the somatosensory cortex were BrdU positive (Figures 7J and 7K), approximately the percentage that one might expect from a 3 hr pulse label with BrdU if all cells in the cortex arose from the *d*CGE itself. These data strongly suggest that bitufted, bipolar, or double bouquet, predominantly somatostatin-negative RSNPs (see Kawaguchi and Kubota, 1996) most likely originate from within the CGE.

Discussion

We have employed ultrasound-guided transplantation of EGFP-expressing ventral neuronal progenitors into wild-type hosts to create a cortical interneuron fate map of the ventral eminences. This study provides a comprehensive characterization of interneuron subclasses derived from the medial (MGE) and caudal (CGE) ganglionic eminences during two critical time windows during neurogenesis. These two progenitor zones show pronounced biases with regard to the subtypes of cortical interneuron that they generate (Table 1). We demonstrate that the spatial and temporal origin of a given progenitor within the ventral telencephalon is a strong predictor of the mature cortical interneuron class that it will give rise to. This in turn suggests that developmental gene expression may be central to the generation of diversity of cortical interneurons.

Interneuron Diversity—Continuum or Distinct Subtypes?

The heterogeneity of cortical interneuron subtypes poses an enormous obstacle to a more thorough understanding of mechanisms of cortical processing and the role that inhibitory networks play in the mammalian brain. The study of cortical interneuron diversity has been approached in a number of ways, focusing both on single- and multiple-cell electrophysiological analyses, immunochemical characterization, and cell expression profiling, as well as detailed morphological reconstructions. Although work in these areas has highlighted some unifying features, it has also produced a bewildering array of classification schemes, which have defied

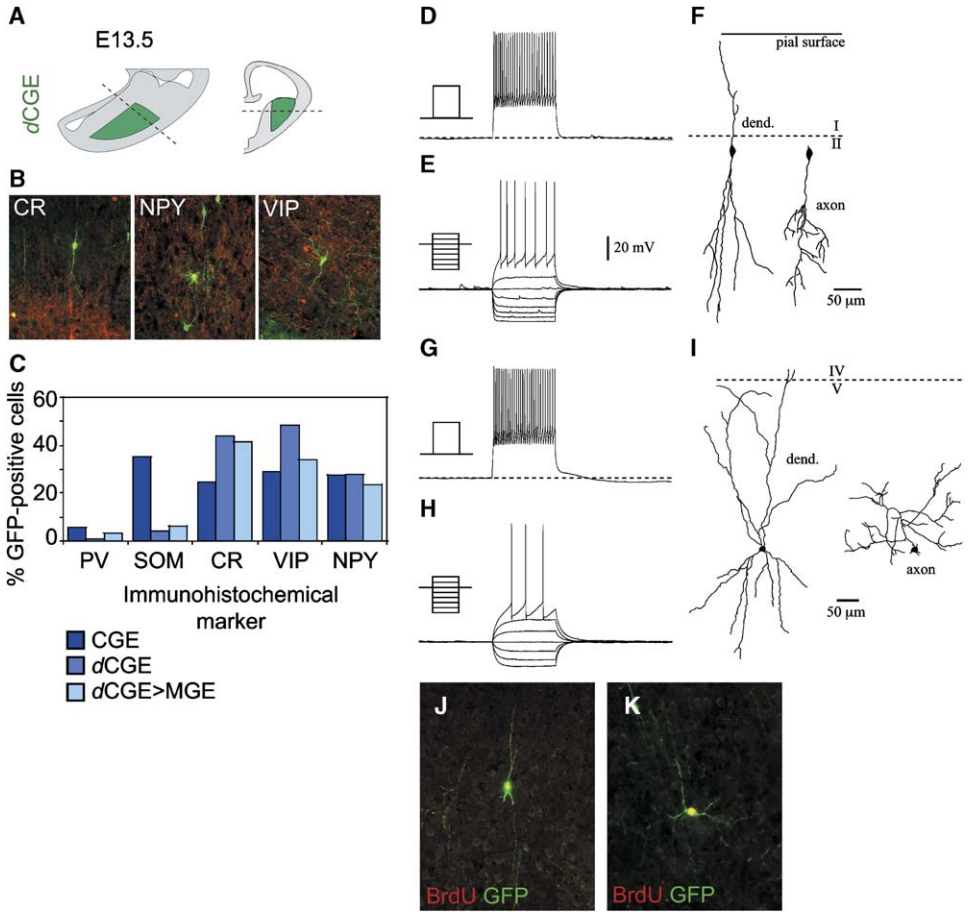

Figure 7. Transplantation of the E13.5 *d*CGE Results in More Discrete Populations of Calretinin- and VIP-Positive RSNP Interneurons

(A) Schematics of the horizontal (left) and coronal (right) sections, illustrating the region termed *d*CGE taken from the ventral telencephalon for in utero transplantation. The dashed lines indicate the position of the coronal and horizontal schematics. (B) Representative immunological stainings and (C) a histogram showing the percentage of GFP-positive cells expressing each immunological marker for the E13.5 CGE, *d*CGE, and *d*CGE heterotopic transplants. The majority of cells from the *d*CGE were CR-, NPY-, and VIP-positive interneurons. This was reflected in the electrophysiological sample that contained a large number of bipolar (D–F), bitufted, and double bouquet RSNP interneurons. (D) Response of a bipolar NR-RSNP to suprathreshold current injection (+100 pA) and (E) to hyperpolarization and near-threshold current injection (initial step, −75pA, 15pA increments). (G) Response to suprathreshold current injection (+240pA) and subthreshold current steps (initial step, −60pA, 20pA increments) of a multipolar RSNP with axon-arcade morphology (I) similar to a VIP-positive population previously published (Kawaguchi and Kubota, 1996). (J and K) Representative stainings of BrdU-labeled bitufted and multipolar *d*CGE-derived cells in the cortex.

simple integration into a single overarching system (Kawaguchi and Kubota, 1997; Markram et al., 2004). Indeed, the seemingly endless array of cortical interneurons has encouraged some to ask whether interneuron diversity can better be thought of as a continuum of cell types (Parra et al., 1998), with each interneuron being a distinct blend of channel makeup, neurochemical expression, layer location, and axonal/dendritic morphology.

Our identification of interneuron subtypes was based on the system proposed by Kawaguchi and colleagues (Kawaguchi, 1995; Kawaguchi and Kubota, 1997), as this provided a comprehensive method of identification that appeared to correlate well with our findings in the mouse somatosensory cortex. However, there were interneurons that diverged sufficiently from the recognized groups previously reported to defy classification by this scheme, and, as such, represented novel classes. Most apparent were the delayed-spiking (DS) interneurons, which although similar to late-spiking (LS) interneurons, were distinct both in their morphology and expression of somatostatin. In addition, we split the broad RSNP class such that we distinguished between cells that exhibited a rebound spike (R-RSNPs) and those that did not (NR-RSNP). This subdivision is similar in part to that observed by Cauli and colleagues (Cauli et al., 2000), who delineated two similar populations of RSNP based on their electrophysiological and molecular analyses (somatostatin and VIP-RSNPs, respectively). It is reasonable to assume that the use of genetically encoded markers will reveal further populations (for example, Blatow et al., 2003).

The E13.5 MGE and CGE Are Distinct Sources of Cortical Interneuron Subtypes

UBM-guided transplantation of EGFP-labeled MGE and CGE progenitors resulted in predictable patterns of migration and cell positioning in the cortex, as previously reported with constitutively expressing placental alkaline phosphatase donor tissue (Nery et al., 2002; Wichterle et al., 2001). Furthermore, recent in vitro work has

Table 1. Source of Cortical Interneuron Subtypes In Vivo

Source	Physiological Class	Proposed Petilla Classification
MGE	FS, parvalbumin-positive basket cell	FS (cFs, dFS.sFS, csFS)
MGE	BSNP, somatostatin-positive, Martinotti cell	cAD
MGE	DS, somatostatin-positive interneuron	Delayed NA-NFS
Early CGE	Dense plexus NR-RSNP	bAD, cAD
Early CGE	Bitufted NR-RSNP	Burst NA-NFS
CGE	Bipolar, calretinin-positive RSNP	Continous NA-NFS
Late CGE	Double bouquet/bitufted rapidly adapting RSNP	iIB

Interneurons were recovered from animals that had undergone either MGE or CGE transplants. Discrete interneuron subtypes were observed to arise from the MGE and CGE, irrespective of the age of the donor tissue. Some neurons were preferentially recorded from either early (E13.5) or late (E15.5) CGE transplants. The right column shows a classification of the interneurons observed in our study, using the nomenclature agreed upon at a meeting of interneuron researchers in Petilla de Aragón in Navarra, Spain. See the text of this article for full descriptions of the physiological classes and the preview by Rafael Yuste (in this issue of *Neuron*) for a description of the Petilla meeting and the new classification system for cortical interneurons.

demonstrated that the spatial-temporal origin of progenitors in the MGE and CGE predict the precise immunocytochemical profiles that we observed in our transplantation studies (Xu et al., 2004). Here, we extended those findings by demonstrating that cells from these ventral regions give rise to distinct subclasses of cortical interneurons. Most strikingly, the MGE seemed to be the sole source of FS, BSNP, and DS interneurons generated at E13.5. MGE-derived FS cells expressed parvalbumin and the potassium channels Kv3.1/Kv3.2. Both whole-cell recording and immunocharacterization using specific FS markers suggested that approximately half of all transplanted E13.5 MGE progenitors became FS interneurons, largely matching their normal abundance in the in vivo rodent cortex. Two other notable populations from these transplants were the BSNP and DS subclasses, which are both associated with somatostatin-positive, Martinotti-like morphologies. It is interesting to note that although RSNP populations were generated from E13.5 MGE transplants, they demonstrated fairly limited diversity, as assessed by immunological and morphological analyses, in comparison with those derived from the CGE (see below).

Despite showing some overlap with E13.5 MGE transplants, the population distribution of CGE-derived cortical interneurons was largely distinct. Most apparent, there were no FS cells produced from the E13.5 CGE progenitor domain, arguing that, at least at this time point, the MGE is the sole producer of this interneuron subtype. Also apparent from these transplants is the preponderance of RSNP interneurons derived from the CGE. In contrast to the relatively uniform population of E13.5 MGE-derived RSNPs, there is a great deal of diversity within CGE-derived RSNPs, including sizeable populations with bitufted, bipolar, and double bouquet morphologies. Furthermore, while the CGE transplants did contain populations of somatostatin cells and, more specifically, BSNP cells with Martinotti-like morphologies, these cell types were largely absent from the *d*CGE transplants. This suggests that these populations are MGE-derived (see below) and were detected in the CGE transplants as a result of caudally directed migration. Moreover, the fact that the fate of *d*CGE cells was not altered by heterotopic transplantation to the MGE argues that the mature character of these cells is intrinsically encoded and largely set when the progenitors become postmitotic (McConnell and Kaznowski, 1991).

Temporal Changes in the Generation of Interneuron Subtypes

Previous work has suggested that interneuron progenitor birth date correlates with the progressive inside-to-outside lamination within the cortical plate (Anderson et al., 2002; Valcanis and Tan, 2003). In addition, the neuronal diversity found between cortical layers implies that ventral progenitor regions could be producing distinct interneuron subtypes at different time points. To further explore this hypothesis, we performed E15.5 CGE transplants and assessed the distribution of mature cortical interneuron fates. Consistent with previous data on temporal lamination of cortical interneurons (Valcanis and Tan, 2003), our E15.5 CGE transplants were biased to the more superficial layers. The majority of CGE-derived cells at E15.5 were RSNP interneurons of a subclass largely distinct from those observed from E13.5 CGE transplants. Surprisingly, the second most prevalent interneuron subclass was found to be the FS basket cell, which at E13.5 was entirely derived from the MGE. This suggests either caudal migration of FS interneuron precursors or a changing developmental competence of the CGE ventricular zone. The latter hypothesis is difficult to reconcile with a transcriptional code model of interneuron cell fate, as the maturing ventral eminences show little anterior/posterior shifting of transcription factor expression domains from E13.5 to E15.5. Two experiments point toward caudal migration of interneuron progenitors before they migrate tangentially into the cortex. E13.5 MGE injections analyzed 2 days later resulted in a large number of cells in the most caudal regions of the ventral telencephalon (Figure S2; see also Yozu et al., 2005), although it is impossible at such early stages to assess what interneuron subtypes these will become. Likewise, BrdU pulse labeling of the E13.5 or the E15.5 ventricular zone prior to *d*CGE or CGE transplantation, respectively, suggests that calretinin-positive neurons, but few parvalbumin- or somatostatin-expressing neurons, are generated from the CGE. Using these three markers as gross divisions for fast-spiking (parvalbumin), RSNP (calretinin), and BSNP (somatostatin) cell types (Kawaguchi and Kubota, 1997), it would appear that neither FS nor BSNP interneurons are generated from the CGE. Furthermore, the E15.5 CGE ventricular zone generated a class of small, calretinin-positive cells that likely correspond to a population uncovered by our electrophysiological analysis.

The extent to which we are able to comment on the temporal changes in the generation of different interneuronal subtypes is limited by our inability to perform E15.5 MGE transplants. In regard to our CGE analysis, it appears that this structure is only able to generate RSNPs and the temporal birth date of progenitors contributes to

subtype diversity within the RSNP class. This may indicate that spatial position is the major determinant of interneuronal class (e.g., RSNP versus FS), while time of origin dictates more specific aspects of their subtype (bitufted, VIP-expressing NR-RSNP versus bipolar, calretinin-positive, rapidly adapting R-RSNP).

Genetics, Interneuron Subtype, and Functional Diversity

Beyond predicting their subtypes, it is interesting to speculate whether the place and time of origin of cortical interneurons determine their differential function in cortical circuits. For instance, several lines of evidence support the hypothesis that the interneuron classes which we believe arise from the CGE subserve specific functional roles in the mature cortex. Specifically, studies in both the neocortex and the hippocampus indicate that some calretinin- and VIP-containing bipolar, bitufted, and double bouquet interneurons selectively innervated each other (forming interconnected webs), as well as other interneurons. Second, these subtypes preferentially target the basal dendrites of pyramidal neurons (Acsady et al., 1996; Gulyas et al., 1996; Peters and Sethares, 1997; Rozov et al., 2001; Somogyi and Cowey, 1981). Considerable work will be needed to achieve a clear understanding of the extent to which developmental genetic programs are responsible for diverse functional cortical units.

The next step toward this goal will be to determine what molecular mechanisms underlie this sorting according to regional and temporal origin. It is likely that the genetic code of transcription factors expressed within the ventral neuroepithelium plays a large role in specifying mature neuronal subtypes. Null mutations of *Nkx2.1* (Sussel et al., 1999 and *Dlx1*/*Dlx2* homeodomain transcription factors (Anderson et al., 1997; Cobos et al., 2005), as well as the proneural gene *Mash1* (Casarosa et al., 1999) have severe effects on cortical interneuron numbers. However, perinatal lethality precludes analysis of changes in specific interneuron subtypes in these mutants. Genetic fate-mapping methods will provide the critical link between embryonic gene expression and mature cortical interneuron identity, while conditional loss-of-function analysis will highlight the importance of these genes. Figuring out the logic by which developmental expression of transcription factors directs mature cortical interneuron identity will likely provide the means to prospectively identify and manipulate specific cortical interneuron populations. We suggest that both the regional expression of specific transcription factors and the developmental progression in gene expression of the progenitor populations are causal in the generation of specific cortical interneuron subclasses.

Experimental Procedures

In Utero Transplantation of EGFP-Positive Donor Cells

Ventricular (VZ) and subventricular (SVZ) zones of the MGE and CGE were dissected from 10–15 mouse embryos expressing EGFP under the β-actin promoter (β-actin^{EGFP} mice) (Okabe et al., 1997), and cell suspensions were prepared for in vivo ultrasound-guided transplantation as previously described (Nery et al., 2002) (Wichterle et al., 1999, 2001). We injected 40–60 nl of the cell suspension into the appropriate eminences of wild-type host embryos. For embryonic analysis of proliferation and migration of transplanted cells, embryos were collected 2 days after transplantation; otherwise all host animals were allowed to go to full term and used postnatally, either for electrophysiology or immunocytochemistry. For the E13.5 and E15.5 CGE BrdU/transplantation schemes, three mothers containing the EGFP donor embryos were given a single BrdU injection (0.5 mg BrdU/10 gm mother) 3 hr prior to sacrifice and removal of EGFP-positive embryos. For analysis of the proliferative status of transplanted progenitors following UBM-guided injection, saturating pulses of BrdU (1 mg BrdU/10gm mother, 3 times every 4 hr) were administered immediately following surgery and at 24 hr and 48 hr postsurgically to three separate E13.5 MGE transplanted mothers.

Electrophysiology

Electrophysiology was performed on mice (P13–P22) that had successfully undergone UBM-guided transplant of neurons expressing EGFP under the β-actin promoter. Animals were anesthetized and decapitated, and the brain was quickly removed and transferred to ice-cold physiological Ringer's solution containing: 125 mM NaCl, 2.5 mM KCl, 25 mM $NaHCO_3$, 1.25 mM NaH_2PO4, 1 mM $MgCl_2$, 2 mM $CaCl_2$, and 20 mM glucose. The brain was then fixed to a stage, and 200 μm slices were cut on a vibratome (VT1000S; Leica Microsystems). Slices were then individually transferred to an incubation chamber containing oxygenated Ringer's solution at room temperature and incubated for a minimum period of 1 hr prior to recording. During recording, slices were continually perfused with oxygenated Ringer's solution of the same composition as that described above.

Whole-cell tight seal recordings were made from EGFP-positive neurons preferentially located in layers 2/3 and 5/6 of the somatosensory cortex. Apart from their location, we randomly selected EGFP-positive profiles typically 40–70 μm below the surface of the slice. Visualization of the fluorescent neurons was achieved via an infrared gradient contrast system and videomicroscopy (Dodt and Zieglgansberger, 1998) (Stuart et al., 1993). Patch electrodes were made from borosilicate glass (resistance, 5–8 MΩ; Harvard Apparatus Ltd., UK) and filled with a solution consisting of: 128 mM K-Gluconate, 4 mM NaCl, 0.3 mM GTP, 5 mM ATP, 0.0001 mM $CaCl_2$, 10 mM HEPES, and 1 mM glucose. For postrecording immunocytochemistry and morphological reconstruction, 0.2% Lucifer yellow was also included.

All recordings were performed in current-clamp mode (Axoclamp 2B; Axon Instruments) and analyzed offline in Clampfit version 9.2. Standard electrophysiological protocols were followed throughout. Passive membrane properties were ascertained shortly after rupturing the patch and periodically during the course of the experiments to ensure that there was no significant deterioration in the health of the cell. Cells that showed significant rundown were discarded. Depolarizing and hyperpolarizing current steps (0.1–0.2 Hz; duration, 500 ms) were applied to the cells to characterize their endogenous electrophysiological profile (see Kawaguchi, 1995). All parameters were measured on at least three occasions for each cell, and the average value was calculated. Input resistances and time constants of the cell were ascertained by passing hyperpolarizing current (≤10 mV step); spike dynamics were measured from the first spike at threshold, and the percentage frequency adaptation was derived from the maximal firing frequency achieved. The latter was calculated as:

$$\% \text{ adaptation} = ((f_1 - f_2)/f_1) \times 100 \quad (1)$$

where f_1 is the frequency in the first 100 ms of the current step and f_2 is the frequency in the last 100 ms (i.e., 400–500 ms). To test whether injection of hyperpolarizing current resulted in rebound spike activity, neurons were typically stepped below −90 mV. To test the threshold spike from a hyperpolarized potential (Kawaguchi, 1995), cells were kept at between −80 mV and −90 mV by constant current injection. Full data sets containing the electrophysiological parameters are provided in the Supplemental Data (Tables S1–S4).

Histological Analysis of Recorded Interneurons

After completion of the electrophysiology, slices containing single Lucifer yellow-filled neurons were transferred to 4% paraformaldehyde and fixed for a maximum of 3 hr at 4ºC under a weighted fine gauze, to prevent distortion of the tissue. Following fixation, they were washed in phosphate-buffered saline (PBS; 0.1 M [pH, 7.2]),

incubated for 20–30 min in 5% sucrose and 0.5% TX-100, and then freeze-thawed to enhance antibody permeability. The slices were then washed again in PBS and blocked with 10% heat-inactivated normal goat serum (NGS) and 0.5% TX-100 for 2 hr. Recorded interneurons were then tested for immunoreactivity to one of three primary antibodies based on the physiological profile of the cell: mouse anti-parvalbumin (1:200; Sigma), rat anti-somatostatin (1:250; Chemicon), or mouse anti-calretinin (1:1000; Chemicon). In all cases, slices were incubated with the primary antibody overnight at 4ºC in 1% NGS/0.5% TX-100. Prior to incubation with the relevant secondary antibody (Cy3 anti-mouse or anti-rat; 1:200), slices were washed thoroughly in PBS. Subsequent to completion, slices were washed once more and then temporarily mounted on well slides for fluorescent imaging (Axioplan 2; Zeiss).

Following the immunocytochemistry, the Lucifer yellow was converted to a dense, dark-colored DAB content to facilitate histological reconstruction. To begin this process, endogenous peroxidase activity was quenched by washing with 1% H_2O_2 in 75% methanol for 20 min after which the slices were washed in PBS and repermeabilized prior to overnight incubation at 4ºC with rabbit anti-LY biotin-XX-conjugated (1:500; Molecular Probes) antibody. After several washes, the tissue was then incubated for an additional night at room temperature with AB reagents (Vector Laboratories Inc., CA) prior to further washes in PBS and development with the DAB reaction for a period of up to 20 min. Slices were then washed and permanently mounted in well slides for camera lucida drawing (magnification ×320). Due to the nature of the slice preparation, axons and dendrites were often severed; however, in the majority of cases distinctive morphological characteristics could be observed.

Tissue Preparation, Histology, and In Situ Hybridization

E13.5 and E15.5 embryos were dissected in cold PBS and fixed in 4% PFA for 4–6 hr at 4ºC. P17 and P20 mice were transcardially perfused and postfixed for 1 hr (for immunohistochemistry) or overnight (for in situ hybridization). All brains were washed in PBS, cryoprotected in 30% sucrose, and embedded in TissueTek on dry ice. Tissues were sectioned serially at 12 μm for double in situ hybridization analysis and at 14–16 μm for all other purposes. Single in situ hybridization was performed as previously described using nonradioactive DIG probes. The cDNA probes used included *Nkx2.1*, *Dlx2*, *Lhx6*, *Cux2*, *ErbB4*, and *SFRP2.*

Immunohistochemistry

The following antibodies were used: chicken anti-GFP (1:2000; Chemicon), mouse anti-BrdU (1:100; Becton Dickinson), rabbit anti-pan-Dlx (1:75; gift of G. Panganiban), rabbit anti-Kv3.1 (1:200; generous gift of B. Rudy), rabbit anti-Kv3.2 (1:250; B. Rudy), mouse anti parvalbumin (1:1000; Sigma), rat anti-somatostatin (1:250; Chemicon), mouse anti-Calretinin (1:1500; Chemicon), rabbit anti-VIP (1:300; Incstar), and rabbit anti-NPY (1:3000; Incstar).

Supplemental Data

Supplemental Data include four tables and three figures and can be found with this article online at http://www.neuron.org/cgi/content/full/48/4/591/DC1/.

Acknowledgments

We are grateful to members of the Fishell lab for comments on the manuscript. We would specifically like to thank Goichi Miyoshi for advice on the BrdU experiments. We are also indebted to Dr. Bernardo Rudy and Ethan Goldberg for discussion, technical advice, and the generous supply of Kv3.1 and Kv3.2 antibodies. We would like to thank Dr. Okabe for the gift of his CAG^{gfp} transgenic mouse. The following people provided cDNA probes and antibodies: J. Rubenstein (*Dlx2, Lhx6*), S. Kimura (*Nkx2.1*), P. Trainor (*Cux2*) and (*ErbB4*), B. Rudy (*Kv3.1*), S. Pleasure (*SFRP2*), and J. Kohtz (pan-Dlx). Finally, we would like to thank Yuan-Yuan Huang and Rebecca Wolsky for excellent technical assistance with transplantations and sectioning. S.B. is a recipient of the Human Frontiers Science Program long-term fellowship. Research in the Fishell lab is sponsored by the National Institutes of Health.

Received: March 9, 2005
Revised: August 18, 2005
Accepted: September 27, 2005
Published: November 22, 2005

References

Acsady, L., Gorcs, T.J., and Freund, T.F. (1996). Different populations of vasoactive intestinal polypeptide-immunoreactive interneurons are specialized to control pyramidal cells or interneurons in the hippocampus. Neuroscience *73*, 317–334.

Anderson, S.A., Eisenstat, D.D., Shi, L., and Rubenstein, J.L. (1997). Interneuron migration from basal forebrain to neocortex: dependence on Dlx genes. Science *278*, 474–476.

Anderson, S.A., Marin, O., Horn, C., Jennings, K., and Rubenstein, J.L. (2001). Distinct cortical migrations from the medial and lateral ganglionic eminences. Development *128*, 353–363.

Anderson, S.A., Kaznowski, C.E., Horn, C., Rubenstein, J.L., and McConnell, S.K. (2002). Distinct origins of neocortical projection neurons and interneurons in vivo. Cereb. Cortex *12*, 702–709.

Blatow, M., Rozov, A., Katona, I., Hormuzdi, S.G., Meyer, A.H., Whittington, M.A., Caputi, A., and Monyer, H. (2003). A novel network of multipolar bursting interneurons generates theta frequency oscillations in neocortex. Neuron *38*, 805–817.

Casarosa, S., Fode, C., and Guillemot, F. (1999). Mash1 regulates neurogenesis in the ventral telencephalon. Development *126*, 525–534.

Cauli, B., Audinat, E., Lambolez, B., Angulo, M.C., Ropert, N., Tsuzuki, K., Hestrin, S., and Rossier, J. (1997). Molecular and physiological diversity of cortical nonpyramidal cells. J. Neurosci. *17*, 3894–3906.

Cauli, B., Porter, J.T., Tsuzuki, K., Lambolez, B., Rossier, J., Quenet, B., and Audinat, E. (2000). Classification of fusiform neocortical interneurons based on unsupervised clustering. Proc. Natl. Acad. Sci. USA *97*, 6144–6149.

Chow, A., Erisir, A., Farb, C., Nadal, M.S., Ozaita, A., Lau, D., Welker, E., and Rudy, B. (1999). K(+) channel expression distinguishes subpopulations of parvalbumin- and somatostatin-containing neocortical interneurons. J. Neurosci. *19*, 9332–9345.

Cobos, I., Calcagnotto, M.E., Vilaythong, A.J., Thwin, M.T., Noebels, J.L., Baraban, S.C., and Rubenstein, J.L. (2005). Mice lacking Dlx1 show subtype-specific loss of interneurons, reduced inhibition and epilepsy. Nat. Neurosci. *8*, 1059–1068.

Dodt, H.U., and Zieglgansberger, W. (1998). Visualization of neuronal form and function in brain slices by infrared videomicroscopy. Histochem. J. *30*, 141–152.

Du, J., Zhang, L., Weiser, M., Rudy, B., and McBain, C.J. (1996). Developmental expression and functional characterization of the potassium-channel subunit Kv3.1b in parvalbumin-containing interneurons of the rat hippocampus. J. Neurosci. *16*, 506–518.

Erisir, A., Lau, D., Rudy, B., and Leonard, C.S. (1999). Function of specific K(+) channels in sustained high-frequency firing of fast-spiking neocortical interneurons. J. Neurophysiol. *82*, 2476–2489.

Flames, N., Long, J.E., Garratt, A.N., Fischer, T.M., Gassmann, M., Birchmeier, C., Lai, C., Rubenstein, J.L., and Marin, O. (2004). Short- and long-range attraction of cortical GABAergic interneurons by neuregulin-1. Neuron *44*, 251–261.

Gonchar, Y., and Burkhalter, A. (1997). Three distinct families of GABAergic neurons in rat visual cortex. Cereb. Cortex *7*, 347–358.

Goulding, M., and Pfaff, S.L. (2005). Development of circuits that generate simple rhythmic behaviors in vertebrates. Curr. Opin. Neurobiol. *15*, 14–20.

Gulyas, A.I., Hajos, N., and Freund, T.F. (1996). Interneurons containing calretinin are specialized to control other interneurons in the rat hippocampus. J. Neurosci. *16*, 3397–3411.

Gupta, A., Wang, Y., and Markram, H. (2000). Organizing principles for a diversity of GABAergic interneurons and synapses in the neocortex. Science *287*, 273–278.

Kawaguchi, Y. (1993). Groupings of nonpyramidal and pyramidal cells with specific physiological and morphological characteristics in rat frontal cortex. J. Neurophysiol. *69*, 416–431.

Kawaguchi, Y. (1995). Physiological subgroups of nonpyramidal cells with specific morphological characteristics in layer II/III of rat frontal cortex. J. Neurosci. *15*, 2638–2655.

Kawaguchi, Y., and Kubota, Y. (1996). Physiological and morphological identification of somatostatin- or vasoactive intestinal polypeptide-containing cells among GABAergic cell subtypes in rat frontal cortex. J. Neurosci. *16*, 2701–2715.

Kawaguchi, Y., and Kubota, Y. (1997). GABAergic cell subtypes and their synaptic connections in rat frontal cortex. Cereb. Cortex *7*, 476–486.

Kiehn, O., and Butt, S.J. (2003). Physiological, anatomical and genetic identification of CPG neurons in the developing mammalian spinal cord. Prog. Neurobiol. *70*, 347–361.

Klausberger, T., Magill, P.J., Marton, L.F., Roberts, J.D., Cobden, P.M., Buzsaki, G., and Somogyi, P. (2003). Brain-state- and cell-type-specific firing of hippocampal interneurons in vivo. Nature *421*, 844–848.

Lavdas, A.A., Grigoriou, M., Pachnis, V., and Parnavelas, J.G. (1999). The medial ganglionic eminence gives rise to a population of early neurons in the developing cerebral cortex. J. Neurosci. *19*, 7881–7888.

Liu, A., Joyner, A.L., and Turnbull, D.H. (1998). Alteration of limb and brain patterning in early mouse embryos by ultrasound-guided injection of Shh-expressing cells. Mech. Dev. *75*, 107–115.

Markram, H., Toledo-Rodriguez, M., Wang, Y., Gupta, A., Silberberg, G., and Wu, C. (2004). Interneurons of the neocortical inhibitory system. Nat. Rev. Neurosci. *5*, 793–807.

McConnell, S.K., and Kaznowski, C.E. (1991). Cell cycle dependence of laminar determination in developing neocortex. Science *254*, 282–285.

McCormick, D.A., Connors, B.W., Lighthall, J.W., and Prince, D.A. (1985). Comparative electrophysiology of pyramidal and sparsely spiny stellate neurons of the neocortex. J. Neurophysiol. *54*, 782–806.

Monyer, H., and Markram, H. (2004). Interneuron Diversity series: Molecular and genetic tools to study GABAergic interneuron diversity and function. Trends Neurosci. *27*, 90–97.

Nery, S., Fishell, G., and Corbin, J.G. (2002). The caudal ganglionic eminence is a source of distinct cortical and subcortical cell populations. Nat. Neurosci. *5*, 1279–1287.

Okabe, M., Ikawa, M., Kominami, K., Nakanishi, T., and Nishimune, Y. (1997). 'Green mice' as a source of ubiquitous green cells. FEBS Lett. *407*, 313–319.

Parra, P., Gulyas, A.I., and Miles, R. (1998). How many subtypes of inhibitory cells in the hippocampus? Neuron *20*, 983–993.

Peters, A., and Sethares, C. (1997). The organization of double bouquet cells in monkey striate cortex. J. Neurocytol. *26*, 779–797.

Reyes, A., Lujan, R., Rozov, A., Burnashev, N., Somogyi, P., and Sakmann, B. (1998). Target-cell-specific facilitation and depression in neocortical circuits. Nat. Neurosci. *1*, 279–285.

Rozov, A., Jerecic, J., Sakmann, B., and Burnashev, N. (2001). AMPA receptor channels with long-lasting desensitization in bipolar interneurons contribute to synaptic depression in a novel feedback circuit in layer 2/3 of rat neocortex. J. Neurosci. *21*, 8062–8071.

Sharma, K., and Peng, C.Y. (2001). Spinal motor circuits: merging development and function. Neuron *29*, 321–324.

Somogyi, P. (1977). A specific 'axo-axonal' interneuron in the visual cortex of the rat. Brain Res. *136*, 345–350.

Somogyi, P., and Cowey, A. (1981). Combined Golgi and electron microscopic study on the synapses formed by double bouquet cells in the visual cortex of the cat and monkey. J. Comp. Neurol. *195*, 547–566.

Somogyi, P., Tamas, G., Lujan, R., and Buhl, E.H. (1998). Salient features of synaptic organisation in the cerebral cortex. Brain Res. Brain Res. Rev. *26*, 113–135.

Stuart, G.J., Dodt, H.U., and Sakmann, B. (1993). Patch-clamp recordings from the soma and dendrites of neurons in brain slices using infrared video microscopy. Pflugers Arch. *423*, 511–518.

Sussel, L., Marin, O., Kimura, S., and Rubenstein, J.L. (1999). Loss of Nkx2.1 homeobox gene function results in a ventral to dorsal molecular respecification within the basal telencephalon: evidence for a transformation of the pallidum into the striatum. Development *126*, 3359–3370.

Valcanis, H., and Tan, S.S. (2003). Layer specification of transplanted interneurons in developing mouse neocortex. J. Neurosci. *23*, 5113–5122.

Wichterle, H., Garcia-Verdugo, J.M., Herrera, D.G., and Alvarez-Buylla, A. (1999). Young neurons from medial ganglionic eminence disperse in adult and embryonic brain. Nat. Neurosci. *2*, 461–466.

Wichterle, H., Turnbull, D.H., Nery, S., Fishell, G., and Alvarez-Buylla, A. (2001). In utero fate mapping reveals distinct migratory pathways and fates of neurons born in the mammalian basal forebrain. Development *128*, 3759–3771.

Xu, Q., Cobos, I., De La Cruz, E., Rubenstein, J.L., and Anderson, S.A. (2004). Origins of cortical interneuron subtypes. J. Neurosci. *24*, 2612–2622.

Yozu, M., Tabata, H., and Nakajima, K. (2005). The caudal migratory stream: a novel migratory stream of interneurons derived from the caudal ganglionic eminence in the developing mouse forebrain. J. Neurosci. *25*, 7268–7277.

Zimmer, C., Tiveron, M.C., Bodmer, R., and Cremer, H. (2004). Dynamics of Cux2 expression suggests that an early pool of SVZ precursors is fated to become upper cortical layer neurons. Cereb. Cortex *14*, 1408–1420.